A Fundamental Study on Conventional Pyrolysis of a Refuse-Derived Fuel

ARTICLE *in* INDUSTRIAL & ENGINEERING CHEMISTRY RESEARCH · APRIL 1995

Impact Factor: 2.59 · DOI: 10.1021/ie00045a010

5 AUTHORS, INCLUDING:

C. Nicolella
Università di Pisa
123 PUBLICATIONS **1,794** CITATIONS
SEE PROFILE

Luigi Petarca
Università di Pisa
45 PUBLICATIONS **1,073** CITATIONS
SEE PROFILE

Mauro Rovatti
Università degli Studi di Genova
49 PUBLICATIONS **862** CITATIONS
SEE PROFILE

Leonardo Tognotti
Università di Pisa
179 PUBLICATIONS **1,996** CITATIONS
SEE PROFILE

A Fundamental Study on Conventional Pyrolysis of a Refuse-Derived Fuel

Valerio Cozzani,† Cristiano Nicolella, Luigi Petarca,† Mauro Rovatti, and Leonardo Tognotti*

Istututo di Scienze e Tecnologie dell'Ingegneria Chimica, Universita' degli Studi di Genova, via Opera Pia n. 15, 16145 Genova, Italy

The pyrolysis behavior of a refuse-derived fuel (RDF) under heating conditions typical of conventional pyrolysis processes was investigated. Thermogravimetric analysis and differential scanning calorimetry were performed on RDF and on some materials which have been considered "key components" of the thermal degradation of RDF. The product fractions obtained by RDF pyrolysis runs in a laboratory-scale fixed bed reactor, at temperatures between 500 and 900 °C, were identified and characterized by different experimental techniques, including gas chromatographic analysis of gaseous products, ultimate analysis, scanning electron microscopy and internal surface area measurements of char. Gas, tar, and char global yields were determined as a function of reactor temperature. The influence of gas-phase secondary tar-cracking reactions on final gas composition was investigated. Overall kinetic parameters obtained by a simple kinetic model are compared to literature data.

Introduction

Solid waste pyrolysis and gasification offer several benefits over conventional disposal means: they provide a captive energy source and reduce the quantity of waste material to be landfilled and the associated cost, the fuel gas and/or liquid may be used in conventional end use systems, and there are minor byproduct and pollutant-generating problems (Buekens and Shoeters,1986).

Among solid wastes, refuse-derived fuels (RDF) constitute a good starting material for pyrolysis and gasification processes, since they present several advantages compared with municipal or other solid wastes, such as relatively constant composition, good transportation and storage possibilities, and the absence of deterioration (Muhlen et al., 1989). These materials are produced by converting the combustible fraction of municipal solid waste (MSW) into a fuel, following mechanical sorting and processing to improve the physical and combustion characteristics of the starting refuse material. Pelletized or densified RDFs undergo further processing to ensure uniform size and weight and increased energy density so that they are suitable feed for conventional boilers and for pyrolysis and gasification. Even if the RDF and the MSW are highly heterogeneous materials, dependent on their country of origin, a recent characterization of the pyrolysis behavior of Italian RDFs, from different MSW feedstocks (Cozzani et al., 1994), has shown that they present the same qualitative behavior. Furthermore, as far as marketing and elemental analysis are concerned, the Italian RDFs studied were found to fall within a quite narrow range of variation.

There is still the need to get fundamental information on devolatilization and pyrolysis of RDFs. These processes are also important for combustion and gasification, the two major routes to be pursued in recovering energy from refuse materials. In fact, the bed region in a MSW or RDF combustor is characterized by relatively low heating rates, inadequate mixing, and low oxygen concentrations, and is typically the site where devolatilization occurs. On the other hand, because of the extremely high volatile content in RDF (up to 85% by weight) pyrolysis is also a very crucial step in gasification processes, where char gasification generally starts when devolatilization and pyrolysis end. As a matter of fact, a detailed pyrolysis/gasification reactor model requires a description of the solid-gas reactions using models of varying degrees of detail to describe the physicochemical phenomena in the neighborhood of and within a RDF particle or pellet. Thus, the topics which should be covered in a fundamental investigation on solid fuel gasification and pyrolysis are primary evolution of volatiles, structure and reactivity of generated char, physical chemistry of the gasification process and related gas characteristics, condensable product formation and related secondary reactions (tar cracking), gas-phase reactions, ash characteristics and handling problems, and emission problems.

Very little data is reported on the gasification and pyrolysis of RDF and other solid wastes. Mallya and Helt (1988) carried out experiments on the pyrolysis of MSW components and RDF pellets in a batch reactor. The liquid reaction products were studied by FTIR, and physical properties were determined. Evans and Milne (1988) used molecular beam mass spectroscopy to study the effects of feedstock composition and process conditions on the products from the pyrolysis of 53 systematically prepared samples of RDFs. They defined six compound classes that can be used to show the range of pyrolysis product variation that is likely to be encountered in larger-scale pyrolysis systems. They also reported the effect on pyrolysis product composition of reactor temperature, moisture content, pellet size, and acid pretreatment. Rampling and Hickey (1988), describing bench and larger-scale studies carried out to obtain fundamental information on the characteristics of RDF and its combustion, pointed out that pyrolysis is an extremely important stage in the combustion of waste and that a rapid surge of volatile evolution takes place around 300-350 °C. Lai and Krieger-Brockett (1992) studied the influence of waste feed properties on the devolatilization rate, composition, and rate of production of RDF pyrolysis products. Other studies refer

* Author to whom correspondence should be addressed.
†Dipartimento di Ingegneria Chimica, Chimica Industriale e Scienza dei Materiali, Universita' degli Studi di Pisa, via Diotisalvi n. 2, 56126 Pisa, Italy.

0888-5885/95/2634-2006$09.00/0

Table 1. Marketing Analysis for RDF Supplied by the Manufacturer and Primary Reacting Species Contents in RDF

a. Marketing Analysis for RDF Supplied by the Manufacturer

material	% in RDF
paper and board	65–70
plastic film	14–16
rigid plastic	1.5–2.5
nonferrous metals, glass, inerts	0.5–1.5
wood, rubber, leather	4–6
other materials (textiles)	8–12

b. Primary Reacting Species Contents in RDF

	% in RDF
cellulose	53
lignin	14
hemicellulose	1
polyethylene	20
inerts	12

to full-scale and pilot-scale RDF or other refuse pyrolysis and gasification plants (Eggen and Kraatz, 1974; Buekens and Schoeters, 1986; Rinker, 1980; Vigil et al., 1980; Ekstrom and Rensfelt, 1988; Rensfelt and Ekstrom, 1988; Murphy, 1989; Stahlberg et al., 1989). These works report information on product yields and characteristics as well as on technological aspects, but generally they lack in analyzing the problems from a fundamental point of view.

The general objective of this study is to gain fundamental information on the pyrolysis of RDF, which may be regarded as a composite material, and to understand the role of its components on its pyrolysis behavior. The aims of the work can be summarized as follows: (1) To identify and quantify the major products of RDF pyrolysis over a wide temperature range. (2) To evaluate the role and influence of the main components of RDF on the characteristics of its pyrolysis products. (3) To characterize gas, tar, and char fractions, in order to better understand the potential applications of RDF pyrolysis and gasification. In particular, the structure and the intrinsic reactivity of the residue char is supposed to influence its eventual gasification. Thus, RDF chars were characterized in terms of surface area and by means of scanning electron microscopy (SEM). (4) To obtain global kinetic parameters for the generation of individual gas products taking into account the vapor-phase tar cracking.

To achieve these goals, an experimental technique providing the quantification of the yields of tar, gases, and char and the closure of material balances has been used, together with thermogravimetric analysis (TGA), differential scanning calorimetry (DSC), and conventional analysis methods. It is expected that the results will assist in the design of versatile gasification/pyrolysis systems suitable for RDF and other types of wastes.

Experimental Section

Materials. A commercial pelletized d-RDF was used in this study. This is an Italian RDF (from the DANECO plant, S. Giorgio di Nogaro, Udine) obtained from MSW (Northern Italian) after several process phases (shredding, air classification, magnetic separation, cyclone separation, mesh screening, and pelletization), which result in a nonputrescible, metal-free material. Tables 1 and 2 report the ranges of variation of marketing composition and the ultimate and proximate analysis, averaged on the basis of characterization of different samples. A previous study on Italian RDFs (Cozzani et al.,1994) has shown that these materials present a quite narrow range of variation, as far as marketing and elemental analysis are concerned.

Table 2. Proximate and Ultimate Analyses of RDF and "Key Components"

%	RDF	paper	wood	PE
humidity	4	4	7	
fixed carbon	9.9	12.8	16.3	0.1
volatile matter	77.8	76.0	81.8	99.7
ashes	12.3	11.2	1.9	0.2
C	45.9	36.00	45.8	84.3
N	1.1	0.10		
H	6.8	5.00	5.9	15.4
O[a]	33.7	47.7	48.1	traces
S	nd	nd		
Cl	traces	traces	traces	traces

[a] By difference.

In spite of some difficulties in interpreting the actual nature and provenance of some categories, it is evident from Table 1 that the RDF consists mainly of cellulosic materials. This is confirmed by the C/H/O ratio of the noninert portion of the MSW that remains in the RDF, which is similar to that of cellulose (Rampling and Hickey, 1988). Wood and plastics (polyethylene terephthalate (PET), polypropylene (PP), and polyethylene (PE)) are also present in the RDF. Interpreting the behavior of the RDF during pyrolysis requires the knowledge of the pyrolysis behavior of the main components of the RDF. From marketing analysis, three "key components" were differentiated as crucial in determining the pyrolysis behavior of the RDF: paper and cardboard, plastics, and wood-like materials. Actual relative fractions of these key components are somewhat uncertain, since it is not easy to find out to which of these components some marketing categories may be attributed. For example, textiles may be either natural or synthetic fibers. In the latter case, their pyrolysis behavior will be similar to that of plastics, otherwise it will be similar to that of cellulosic materials.

In order to compare the behavior of the RDF and key components during pyrolysis, different well-characterized materials were selected for TGA and DSC runs. As representative of the paper and cardboard fraction, a mixture of 80% by weight of newsprint paper and 20% of bond grade writing paper was used. Pure high-density polyethylene (HDPE) and a mixture of 50% by weight of poplar and pine sawdust were used respectively for the plastic and wood-like fraction. Ultimate and proximate analyses of these materials are reported in Table 2. The criteria followed to select materials used as representative of the RDF key components were mainly based on characteristics of the MSW fed to the RDF production plant (supplied by the manufacturers) and results of RDF ultimate analysis. The absence of poly(vinyl chloride) in the plastic fraction of the RDF used in this work is suggested by the very low chlorine content shown by ultimate analysis. Polyethylene seems to be the plastic material present in greater amount in the RDF, as shown by marketing analysis reported in section a of Table 1, and was used in this work as representative of the pyrolysis behavior of the plastic components of the RDF. However, experimentally determined pyrolysis behaviors of other plastics that may be present in the RDF in minor amounts (PET and PP) are quite similar to that of PE, at least for the temperature–weight loss history (Grassie and Scott, 1985). A 50% mixture of pine and poplar sawdust was

used as representative of wood-like materials because, referring to cellulose, hemicellulose, and lignin content, pine wood is a typical resinous wood, while poplar is a typical "hardwood" and is widely present in MSW, due to its use in fruit boxes and plywood.

RDF components are only grossly mixed in commercial pellets. As relatively small samples were used in the experiments, in order to enhance the reproducibility of experimental data and to minimize sample heterogeneities, the RDF and key components were previously frozen in liquid nitrogen and milled to obtain fine powders. Even if RDF milling to obtain fine powder may be questionable, the use of small pulverized samples eliminates the influence of mass transfer on the observed experimental kinetics.

Experimental Techniques. In order to study the thermal degradation of RDF, three laboratory techniques have been used: thermogravimetric analysis (TGA), differential scanning calorimetry (DSC), and a fixed bed reactor (FBR).

1. TGA and DSC. In TGA runs, RDF pyrolysis was studied by measuring weight loss histories of samples subjected to well-defined heating conditions in an inert atmosphere of pure nitrogen. Weight loss curves during RDF pyrolysis were obtained in both isothermal and constant heating rate conditions. A Mettler TA-3000 system was used. TGA and differential thermogravimetric (DTG) curves were recorded for two different heating rates (10 and 20 °C/min), typical of conventional pyrolysis reactors and of FBR runs. Pure nitrogen was used as an inert purge gas, both to prevent the presence of air in the pyrolysis zone and to remove gaseous and condensible products evolved during pyrolysis, thus minimizing secondary interactions with the hot solid residue. A constant flow rate of 0.1 N L/min was fed to the apparatus.

Isothermal TGA curves were obtained by inserting RDF samples within the preheated TGA furnace. Small samples (less than 30 mg), held on a stainless steel wire net, were used. The wire mesh size prevented char from falling through the net. A pure nitrogen flow (0.15 N L/min) was present to prevent sample oxidation and to remove gaseous pyrolysis products. Temperature transients due to sample heating from ambient to furnace temperature were calculated accounting for convective and conductive heat transfer between the cylindrical furnace and the sample. The Biot number of the sample in these conditions is about 10^{-2}, so that the sample can be considered isothermal. The characteristic time of the system (RDF + sample holder in the TGA), defined as $\tau = mC_p/h$ (where m is the total mass of the system, C_p is the mean specific heat, and h is the heat transfer coefficient), was of the order of 20 s. This time, compared to a total time of 30 min for the experimental runs to be completed, provides that the weight losses during the sample heating are almost negligible, at least at temperatures lower than 600 °C.

DSC was used to measure heat generation or absorption during the thermal degradation processes involved. DSC curves at a constant heating rate (10 °C/min) have been recorded using a Mettler DSC-25 calorimeter. The typical sample weight was less than 6 mg. Golden crucibles were used to allow temperatures up to 750 °C. Pure nitrogen was also used as a purge gas in these experiments. The RDF, papers, and plastic powders were pressed into small discs for calorimetric measurements.

All samples used in TGA, isothermal, and DSC runs were previously dried at 110 °C for 10 h in an inert atmosphere of pure nitrogen.

2. Fixed Bed Reactor. A fixed bed reactor (FBR) method was used for pyrolysis runs on beds of RDF (Figure 1, Table 3). A tubular reactor, fluxed by a helium stream, was used to produce a sufficient amount of gases to be semicontinuously collected and characterized by gas chromatography. The reactor consisted of a Inconel inner tube mounted coanularly within the furnace refractory. Milled RDF was supported in a stainless steel cylindrical wire-mesh basket. The dimensions of the basket (see Table 3) were chosen in order to have a length/diameter ratio greater than 5. This allows us to neglect the end effects and to model the system as a one-dimensional cylindrical reactor where only radial gradients are present. The temperature of the gas stream, T_G, and that in two positions (center, T_C, and wall, T_W) within the fixed bed were continuously recorded by means of J type thermocouples (1.8 mm diameter).

Reactor characterization was carried out in order to evaluate the gas temperature profiles and the heat-exchange coefficient in conditions of gas flow typical of the pyrolysis runs (Bergui, 1994). The characteristic bed heating time, evaluated by using a bed of glass beads, was of the order of 10−20 min (that means heating rates of 0.5−1.5 °C/s) . Measurements of the gas temperature along axial and radial coordinates were also performed. The gas bulk temperature was slightly below the programmed furnace temperature (less than 20 °C), due to heat transfer limitations. The temperature variations along axial and radial coordinates were less than 10 °C.

The experimental procedure was as follows: At the beginning of each run, about 15 g of the RDF was fed into the basket; care was taken in distributing the solid material uniformly within the basket. The reactor was preheated at the temperature chosen for the experimental run, with furnace temperatures ranging between 500 and 900 °C. The basket was left in a pure helium stream before insertion in the reactor, in order to sweep out air, thus preventing oxidation during insertion in the hot reactor. A 1 N L/min flow of inert carrier gas (helium) was used. RDF bed heating rates in these experiments (0.5−1.5 °C/s, see Figure 5) are typical of conventional pyrolysis processes. Reaction times of about 60 min were needed to allow complete conversion of the RDF.

Due to its geometry, this system allows also gas-phase reactions to occur, since a hot tubular reactor section is present after the fixed bed (see Figure 1). The gas residence time can be modified by changing the length of the sample holder. In these experiments, a length of 350 mm was used, so that the gas mean residence time in the "homogeneous" section was evaluated to be of the order of 6−22 s, depending on the operating temperature and on the rate of volatiles production.

Products Recovery and Analysis. Upon exiting the reactor, volatile products pass through a tar trap consisting of a reservoir maintained at 60−70 °C; after the warm trap, the products pass through two cold traps (≈ 0 °C); and finally the uncondensed gases are sampled in a six-reservoir system with gas-sampling valves. Samples are collected at known times for gas chromatographic analysis.

This system provides four different fractions to be separated and recovered from RDF pyrolysis. In this study these fractions are operationally defined as (1)

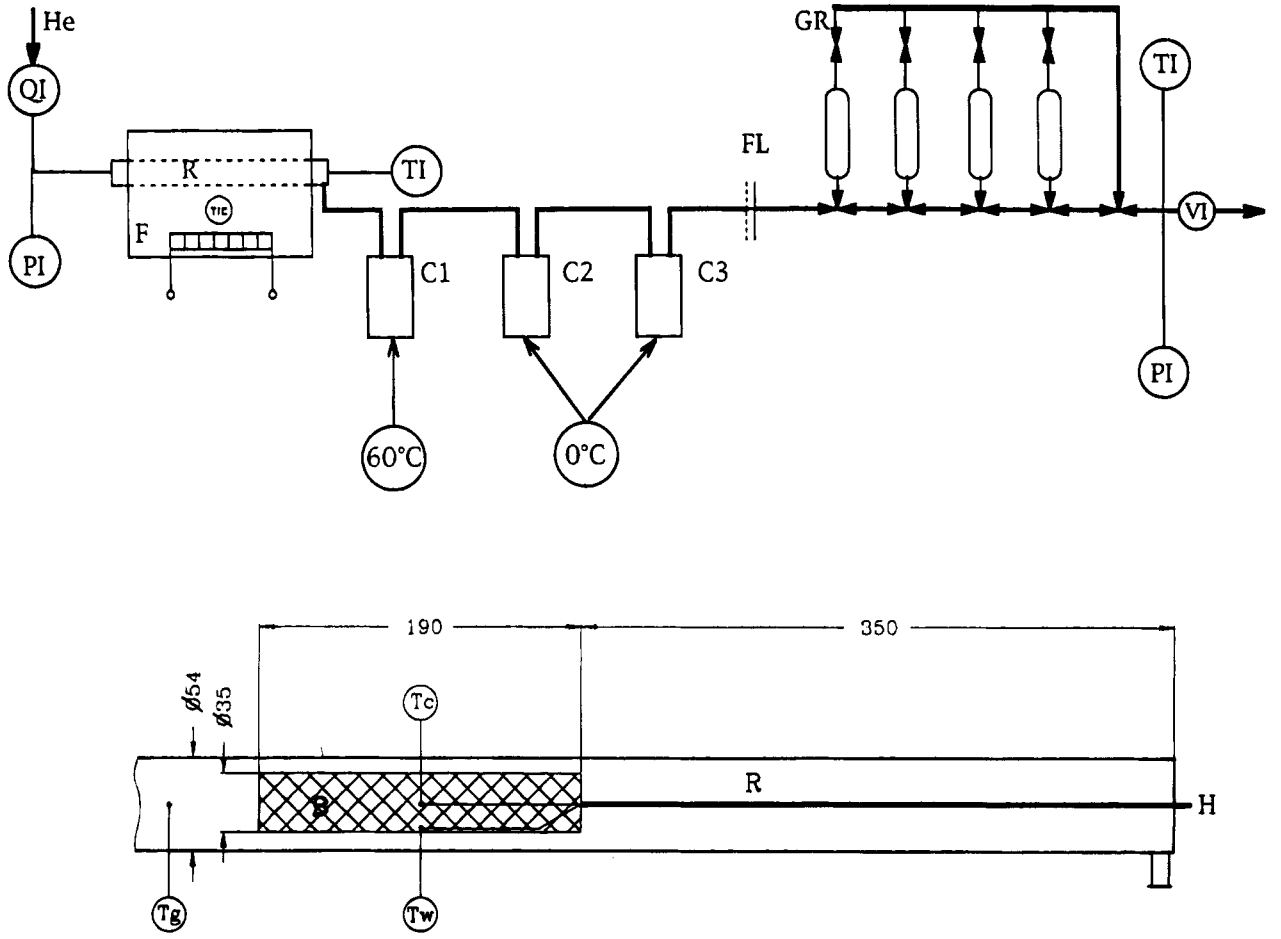

Figure 1. Schematic of the fixed bed reactor and of the product recovery system: B, basket; C1, high-temperature trap; C2 and C3, low-temperature traps; F, furnace; FL, filter; GR, gas reservoirs; H, thermocouple holder; PI, pressure indicator; QI, flow meter; R, tubular reactor; T_C, T_G, and T_W, thermocouples; TI, temperature indicator; VI, gasmeter. All dimensions are in mm.

Table 3. Experimental System Characteristics

reactor (R)	
internal diameter	54 mm
length	1000 mm
L	350 mm
material	inconel alloy 600 FAA 1323/01
RDF basket (B)	
internal diameter	35 mm
length	190 mm
material	stainless steel wire mesh
furnace (F)	
TZF Carbolite Furnaces	
carrier gas	
helium	0.9−1.1 L/min
GC system	
Perkin Elmer Sigma 2B	
column	chromosorb 102 + silica gel
detector	TCD

char, the solid fraction remaining in the basket at the end of the run; (2) tar, the organic volatile material that is recovered from the warm tar trap and other piping system surfaces; (3) water, the aqueous solution that is recovered from the cold traps and that is unmixed with tar in the other trap and tubings; and (4) gas, what is not condensed in the trap system.

The total gas volume was measured continuously by means of a gas counter at the end of the line. Subtracting the carrier gas flow rate, which was measured by a flow meter before the reactor, from the total gas flow rate evaluated at the end of the line, it was possible to obtain the production rate of pyrolysis gases.

A Perkin Elmer Sigma 2B gas chromatograph was used to analyze the contents of each gas sampling loop for carbon monoxide, hydrogen, carbon dioxide, methane, acetylene and ethylene, ethane, and C_3 hydrocarbon gases. GC columns and detector characteristics are reported in Table 3. These assays, together with the overall gas flow rate, allowed us to determine the rate of product evolution, averaged over the time required to fill the gas sampling reservoir (about 30 s). Integration of these rates over the experimental run time allowed the cumulative yields of individual gases to be determined.

Tar and water yields were determined by weighing the traps and all tubings in the reactor system before and after every experimental run and by separating the aqueous solution from the tar phase. Washing of traps and substitution of tubings were carried out after each run.

The char fraction was extracted from the basket at the end of the run and weighed. Further characterization of char fraction included ultimate analysis, evaluation of internal surface area (Carlo Erba S2000 mercury intrusion porosimeter and Quantachrome Quantasorb Q10), and structure analysis by scanning electron microscopy (SEM).

Results and Discussion

TGA and DSC. TGA and DTG curves at constant heating rates obtained for the RDF and key components are reported in Figure 2 parts a and b. Two main

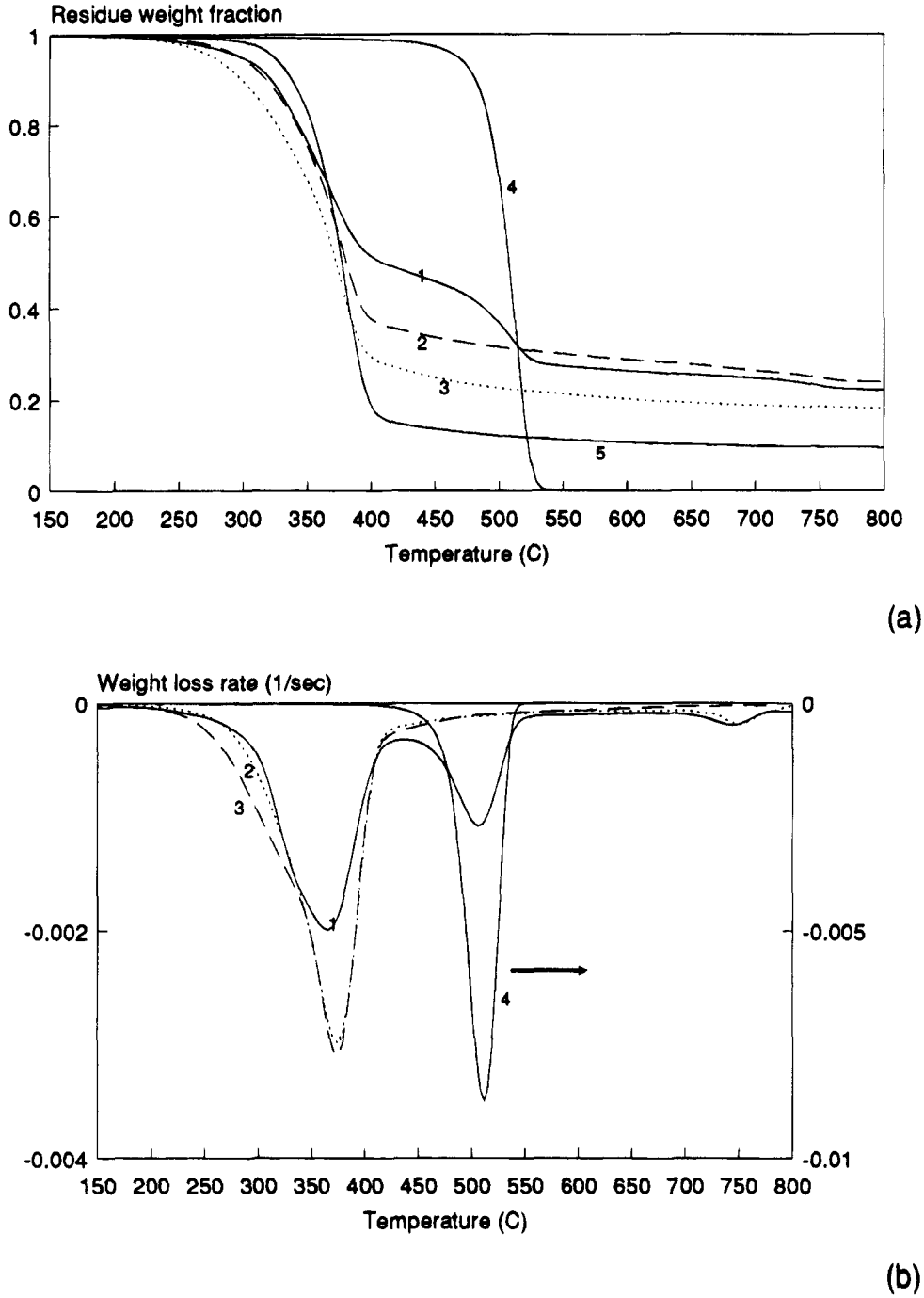

Figure 2. Constant heating rate TGA (a) and DTG (b) curves in N_2 for RDF and "key components". Heating rate 20 °C/min. 1, RDF; 2, paper; 3, wood; 4, polyethylene; 5, α-cellulose.

distinct weight loss steps characterize the curve obtained for the RDF, the first in a temperature range between 300 and 400 °C and the second between 450 and 500 °C. Qualitative pyrolysis behavior and temperature ranges for the first and second degradation steps are in good agreement with data present in the literature for other RDFs (Rampling and Hickey, 1988). Figure 2b points out the striking correspondence of the temperature range of the first and second degradation peaks of the RDF with those of cellulosic materials (paper and wood) (Roberts, 1970; Agrawal et al., 1984; Koufopanos et al., 1989) and of plastics (polyethylene) (Madorski, 1952; Jellinek, 1949; Oakes and Richards, 1949), respectively.

Isothermal TGA curves, obtained with the RDF in pure nitrogen at different temperatures, are reported in Figure 3. It can be seen that the char yield (weight fraction of residue solid) decreases as the temperature increases. At temperatures higher than 500 °C the char yield is around 23% and is almost independent of temperature. This yield is quite low, considering that the residue weight fraction includes the 12% inerts initially present in the RDF. The broad difference in the final char yields obtained at 385 and 500 °C (45% vs 23%) is probably mainly due to the degradation of plastic components, which starts at temperatures higher than 450 °C. This hypothesis is confirmed by the constant heating rate TGA curve of Figure 2a for the RDF. The 20% weight loss recorded between 400 and 500 °C is comparable to the difference in final solid residue obtained from isothermal TGA curves and is in the temperature range of polyethylene degradation.

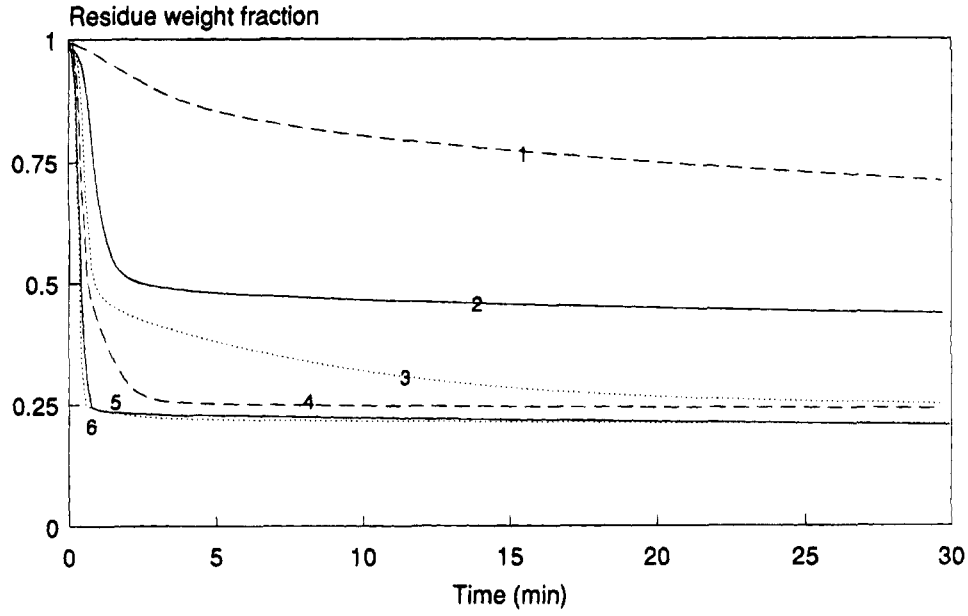

Figure 3. Isothermal weight loss TGA curves in N_2 at various temperatures for RDF: 1, 300 °C; 2, 385 °C; 3, 450 °C; 4, 500 °C; 5, 600 °C; 6, 700 °C.

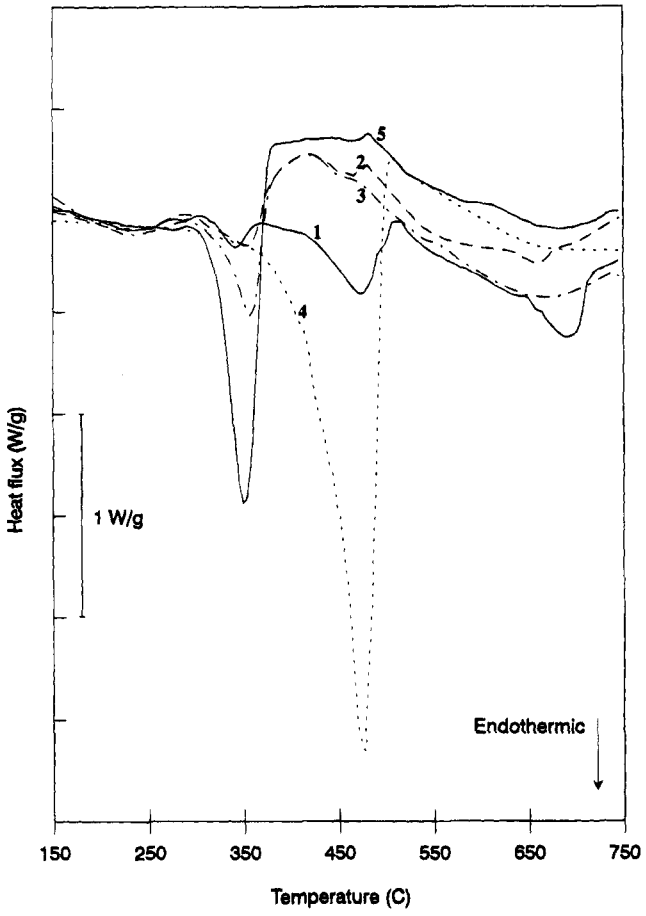

Figure 4. DSC curves in N_2 for RDF and RDF "key components". Heating rate 10 °C/min. 1, RDF; 2, paper; 3, wood; 4, polyethylene; 5, α-cellulose.

Figure 4 reports the DSC curve obtained for the pyrolysis of the RDF and key components in pure nitrogen at a heating rate of 10 °C/min. It must be remarked that samples undergo weight losses during heating. The curves for biomasses are in good agreement with previous data reported in the literature for wood pyrolysis (Capart et al., 1985). The energetics of the pyrolysis reaction of biomasses (plastics pyrolysis is endothermic) is still uncertain: endothermic as well as exothermic data have been reported in the literature. This ambiguity is believed to be due to the contemporary presence of endothermic primary reactions and of exothermic secondary reactions (see Koufopanos et al., 1991; Di Blasi, 1993). At low temperatures and short residence times of volatiles, only primary endothermic reactions occur, while at high temperature and high residence times of volatiles secondary exothermic reactions are also present. However, the reactions occurring in a DSC run may be regarded as low-temperature, primary reactions since a low heating rate was used and a purge gas flow was present in order to sweep off the volatiles that escaped from the crucible.

The RDF curve is characterized by three endothermic peaks caused by degradation reactions. A comparison with the DTG curve shows that the endothermic peaks of the DSC curve are in the same temperature range as the first and second peaks of the DTG curve, so that they are attributable to the endothermic degradation of cellulosic materials and plastics, respectively. The third endothermic peak probably results from the thermal degradation of mineral matter, such as calcium carbonate, widely used as inorganic filler in paper manufacture. Figure 4 also shows the DSC curves for key components and α-cellulose. When the first peak of the RDF curve is compared to that of α-cellulose, thermal effects of RDF pyrolysis can be considered negligible. Furthermore, the DSC curve of paper shows an endothermic peak practically coincident, both in magnitude and temperature range, with the first peak of the RDF. Finally, the temperature range of the second endothermic peak in the DSC curve of the RDF corresponds quite well to that of polyethylene thermal degradation.

The heats of reaction have been calculated for the first and second endothermic degradation peaks of the RDF; the average values were $\Delta H_{R1} = 70$ J/g and $\Delta H_{R2} = 121$ J/g, respectively. Both values are referred to the sample's initial weight. The calculated values of the heats of reaction show that thermal effects of RDF pyrolysis reactions are relatively minor. Further insights into these DSC data may be achieved by considering RDF weight losses together with actual fractions

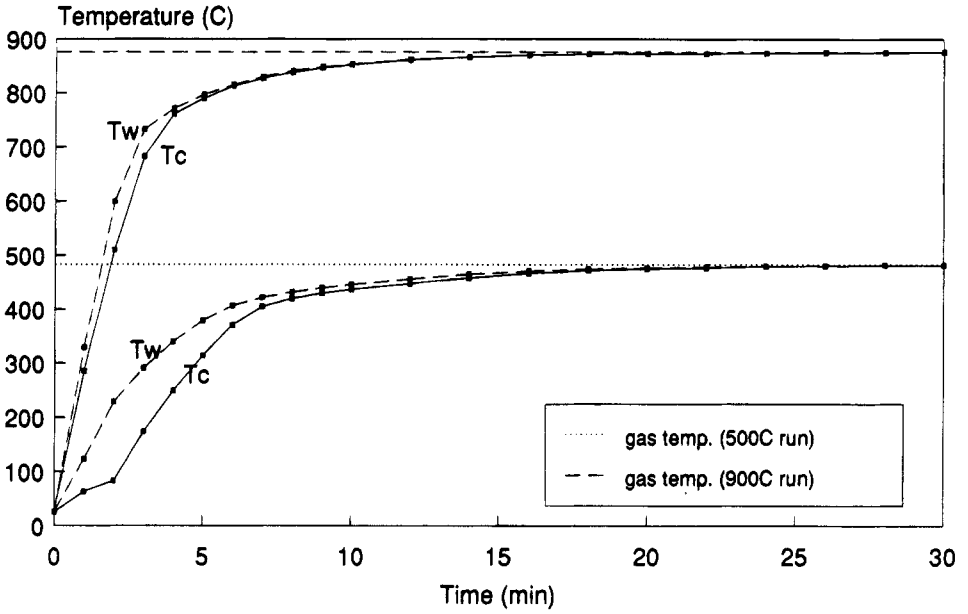

Figure 5. Fixed bed reactor: RDF bed central (T_C) and wall (T_W) temperatures versus time during pyrolysis for different furnace temperatures (500 and 900 °C).

of key components in RDF, as reported in section b of Table 1. The components that actually undergo degradation reactions during the first and second DSC peak seem to be cellulose, hemicellulose and lignin (that sum up to 68% of the initial weight of the RDF) and plastics (20% of the initial weight of the RDF), respectively. Considering only the weight fraction of the components that actually undergo degradation reactions, the values of the heats of reaction are $\Delta H_{R1} = 120$ J/g and $\Delta H_{R2} = 605$ J/g. The second value is comparable with the value obtained from DSC data for pure PE, $\Delta H_{PE} = 650$ J/g.

Comparison of TGA and DSC data for the RDF and its components demonstrates quite well that the behavior of the RDF during pyrolysis may be considered somehow as the sum of the separate behaviors of each key component, at least under TGA and DSC conditions. This statement will be further considered in the analysis of the FBR data.

FBR Product Yields. The temperature–time histories of the RDF bed for two pyrolysis runs, at furnace temperatures of 500 and 900 °C, respectively, are reported in Figure 5 (in the following, the furnace temperature will be used to identify the run). The temperature gradient between the center and the wall of the RDF bed was always less than 100 °C.

Figure 5 also shows how the moisture content (4%) influences the solid-phase temperature profile. There is a temperature inflection near 100 °C, due to moisture evaporation. As previously reported by other investigators (Lai and Krieger-Brockett, 1992), moisture in the feedstock simply results in a delay in the temperature rise but does not influence the ultimate temperature attained if the heating rate is sufficiently high and the heating time sufficiently long. Thus, moisture delays the gas evolution but does not substantially change its composition.

Figure 6 shows the cumulative gas production (a) and gas release rates (b) versus time as a function of the furnace temperature. The cumulative gas yield increases with the furnace temperature. The gas evolution from the sample subjected to the most drastic conditions (the higher the furnace temperature, the greater the heat flux to which the sample is subjected) is seen to occur with a sharper, earlier peak. When temperature profiles, gas release rates, and mass losses (TGA) are compared, it can be seen that the maximum rate of gas production is generally attained when the RDF bed temperature is between 450 and 550 °C. This implies that the pyrolysis of RDF is almost completely ended at 550 °C. The different gas yields and compositions found by raising the furnace temperature are mainly due to the increasing amount of homogeneous tar-cracking products and to gas-phase reactions present at higher furnace temperatures.

Figure 7 reports the results of a mass balance calculation for the four different fractions recovered as a function of furnace temperature. The gas mass fraction is calculated by evaluating the average molecular weight of uncondensables by gas analysis data (see later) and by considering the gas production on a mass basis from the volumetric gas flow rates. The mass balance in the present experiments was better than 96%. Most of the discrepancy was perhaps due to the drift of fines from the basket reactor and to incomplete recovery of volatiles condensed at the end wall of the tubular furnace.

Figure 7 also shows that the char yield is quite low, as already pointed out while discussing Figures 2a and 3: at temperatures higher than 500 °C, it ranges within 20%–25% of the initial weight of the RDF. It must also be considered that virgin RDF contains 12% inerts, which result in a char having more than 40% inert materials. The low char yield and the high volatile content also point out the crucial role of the pyrolysis stage in gasification processes.

The yields of both aqueous and nonaqueous liquid phases are highly dependent on the gas temperature in the range 600–900 °C, as shown in Figure 7. The tar fraction ranges from about 40% of the initial mass at 500 °C to 28% at 900 °C. The water fraction is around 10% at a furnace temperature of 500 °C, while it decreases to about 4% at higher furnace temperatures. Water recovered at the end of the high-temperature runs (800–900 °C) is mainly due to the initial moisture content of the RDF (4%), since water vapor–solid phase interactions are ineffective at the temperatures at which moisture is released; on the other hand, most of the water vapor released by the degradation of organic

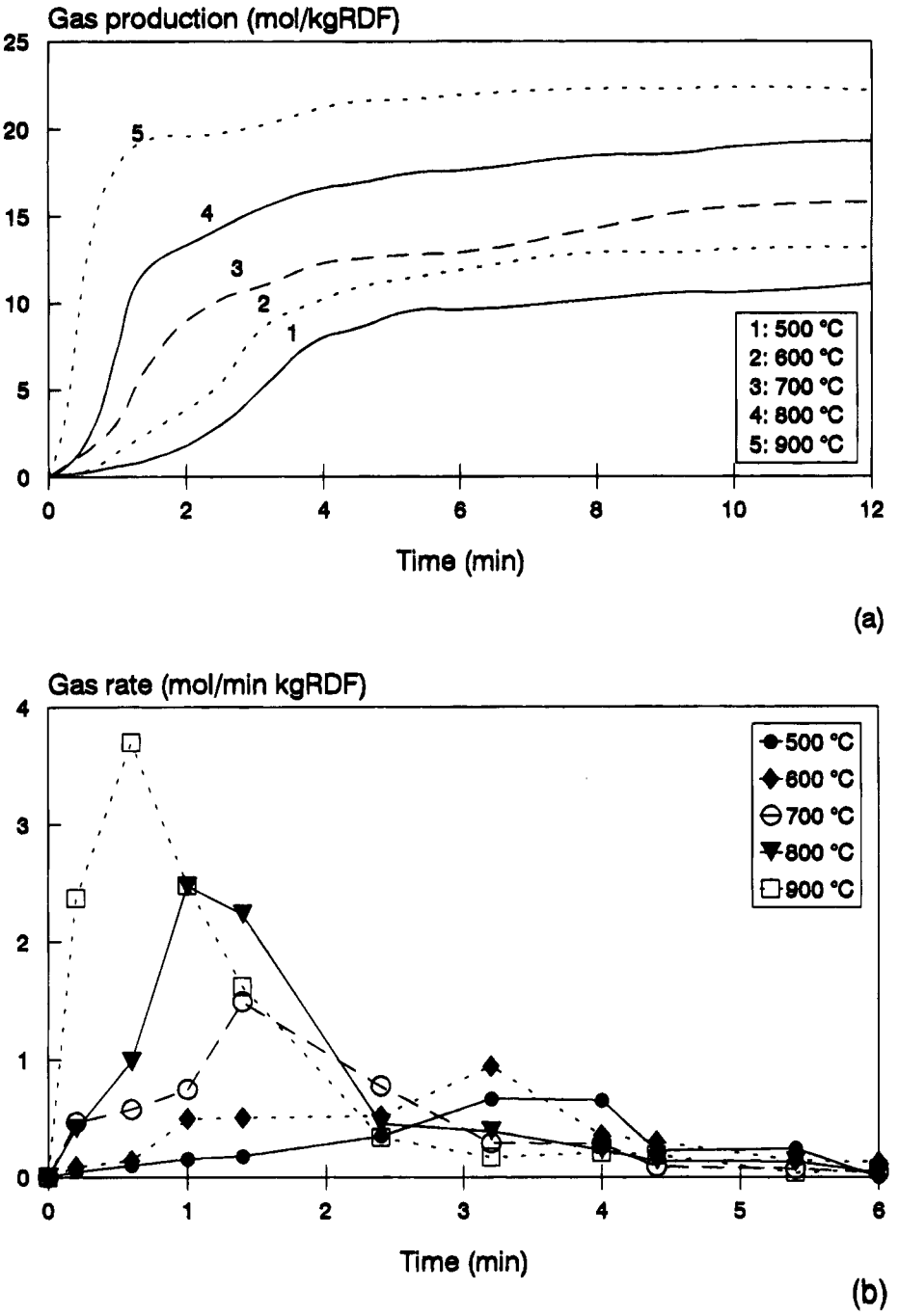

Figure 6. Fixed bed reactor: (a) cumulative gas production and (b) gas production rate versus time as a function of furnace temperature.

constituents at a temperature higher than 500 °C is supposed to take part in the complex gas-phase interactions involving other volatile products. Both tar and water yields decrease with temperature, as generally found in the literature as far as biomass pyrolysis is concerned (Hajaligol et al., 1982; Antal, 1983; Antal, 1985; Chan et al., 1988; Scott et al., 1988; Kojima et al., 1991; Evans and Milne, 1987). This depletion is associated with the noticeable increase of the gas fraction starting from furnace temperatures of about 600 °C and is mainly due to homogeneous gas-cracking reactions which convert the high molecular weight condensables into gaseous compounds of lower molecular weight. However, the ultimate value of the tar yield at 900 °C (28%) is much greater than the values found in the literature (Boroson et al., 1989) for wood (4.77%–5.79%). This may be due to the fact that RDF tars are produced by different primary reacting components: the RDF used in this work contains 5%–10% wood only, and about 20% plastics (mainly PE). The literature on polymer thermal decomposition over this temperature range reports that the major pyrolysis products are low or high molecular weight tars rather than gases (Sugimura and Tsuge, 1979; Hodgkin et al., 1982; Iida et al., 1975; Khalturinskii, 1987), thus the presence of plastics in the RDF results in a greater tar yield and a lower gas yield than what is generally found for biomass pyrolysis.

It has been shown, by comparing TGA and DSC data, that the behavior of the RDF during pyrolysis may be considered somehow as the sum of the separate behaviors of each key component. Thus, the rate of thermal degradation of the RDF can be considered as the sum of the rates of the main RDF components: paper, consisting mainly of cellulose; wood-like materials, composed mainly of cellulose, lignin, and hemicellulose;

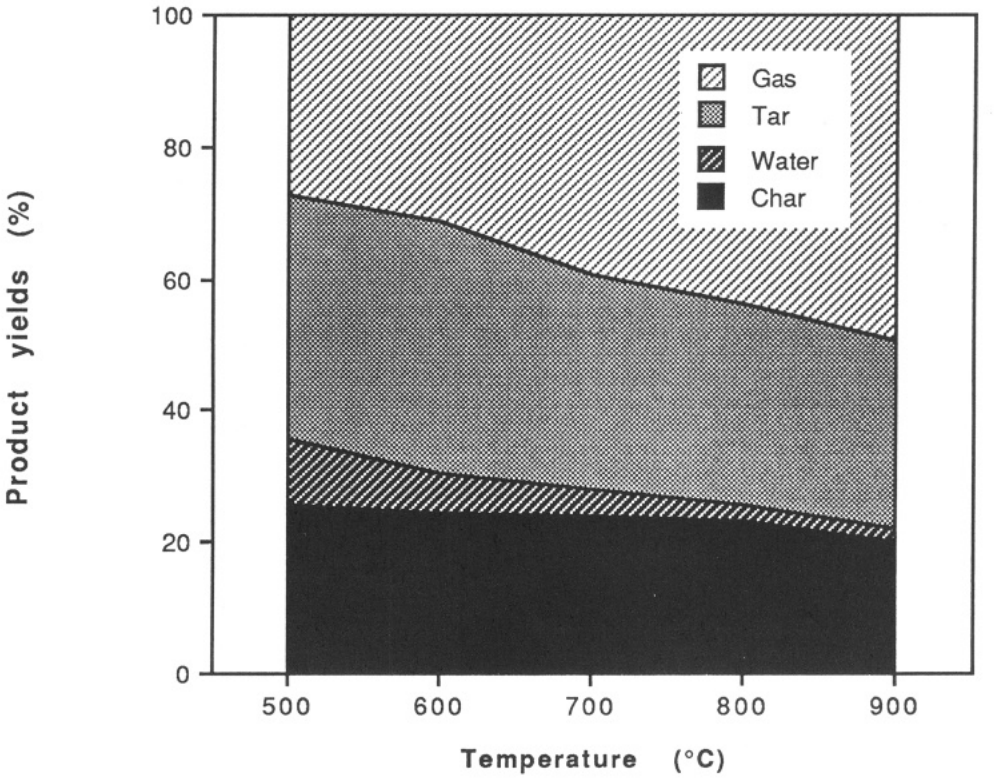

Figure 7. Fixed bed reactor: cumulative products yields versus furnace temperature (mass basis).

and plastics, in this case mainly PE. In previous papers (Ward and Braslaw, 1985; Koufopanos et al., 1989; Cozzani et al., 1994) it was also assumed that each of the "primary reacting species" (i.e., cellulose, lignin, hemicellulose, and PE for RDF) contributed to the formation of this sum to an extent proportional to its contribution to the composition of the RDF. The assumption is made that no interactions occur between RDF components during pyrolysis. Even though this hypothesis is not fully verified, it is clear that possible interactions between RDF components have a negligible effect on the RDF global behavior during pyrolysis, at least as far as weight decrease due to solid-phase degradation reactions is concerned. The simplified description of RDF pyrolysis behavior resulting from this approach also may allow product yields to be estimated on the basis of literature data on the pyrolysis behavior of the above-mentioned "primary reacting species" present in the RDF. The literature reports a staggering amount of data on the pyrolysis of biomasses. While the char yield is mainly dependent on the starting material (since generally biomasses contain different amounts of cellulose, hemicellulose, and lignin), it seems difficult to draw general conclusions on the dependence of volatile product yields (gases, tar, and water) on temperature for each species, since yields critically depend on reactor operating conditions (heating rates and residence times). However, it is possible to verify whether product yields found in this work are comparable with those obtained in the literature data on the pyrolysis of the above-defined "primary reacting species". It should be noted that this comparison has to be made between data obtained in a temperature range for which homogeneous tar-cracking and gas-phase reactions are not active (T < 600 °C), since these latter phenomena are strongly dependent on the reactor operating conditions as far as conventional pyrolysis is concerned (slow heating rates and long residence times). For temperatures of 500−600 °C, cellulose generally produces 10−15% char, 45−55% liquid products (tar and aqueous solution), and 30−35% gases; lignin pyrolysis gives 28−30% char, 30% liquid, and 40−42% gases (Maschio et al., 1992; Bilbao et al., 1987; Bilbao et al., 1989). Finally PE produces mostly tars (Sugimura and Tsuge, 1979; Hodgkin et al., 1982). Hemicellulose is not taken into account since its content in the RDF is very low (see section b of Table 1). By using the coefficients c_j reported in section b of Table 1, the global yields can be calculated simply as

$$Y_{\mathrm{RDF},i} = c_1 Y_{\mathrm{cell},i} + c_2 Y_{\mathrm{lign},i} + c_3 Y_{\mathrm{PE},i} \qquad (1)$$

where the subscript i refers to the char, gas, and liquid, respectively; yields of 25% char (12% + 12.3% inerts), 50% liquids, and 25% gas are obtained. These values are in good agreement with the experimental findings at 500 °C (see Figure 7).

It should be noted that the conclusion that the pyrolysis of RDF appears to be the superposition of the pyrolysis of its components, as TGA, DSC, and FBR data seem to confirm, is likely to hold only for the conditions of the present study, i.e., small samples of milled RDF (where volatiles escape before secondary heterogeneous reactions) and low heating rates. For larger particles and faster heating this statement may fail.

Product Characterization. 1. Char. Char samples obtained by FBR runs in the temperature range 500−900 °C were fully characterized in order to evaluate the effect of the furnace temperature on the char composi-

Table 4. Ultimate Analysis of Char from FBR Runs

%	450 °C	500 °C	600 °C	700 °C	800 °C	900 °C
C	49.2	47.9	48.1	48.6	45.8	49.7
N	1.7	1.6	1.7	1.9	1.3	1.0
H	2.2	1.4	1.3	1.3	0.8	0.5
O[a]	14.5	8.8	9.2	10.7	11.1	6.0
ashes	32.4	40.3	39.7	37.5	40.9	42.9

[a] By difference.

Table 5. Gas Composition at Different Furnace Temperatures

furnace temperature (°C)	gas composition													
	CO		CO_2		H_2		CH_4		C_2H_4, C_2H_2		C_2H_6		C_3H_6	
	% V	% M	% V	% M	% V	% M	% V	% M	% V	% M	% V	% M	% V	% M
500	63.1	73.0	11.6	19.1	17.5	1.5	5.5	3.7	1.5	1.8	0.8	1.0	0.0	0.0
600	46.5	62.5	12.2	23.5	29.4	2.8	8.6	6.6	1.4	1.9	2.0	2.8	0.0	0.0
700	35.9	49.2	13.1	25.5	31.4	3.1	8.5	6.7	8.2	11.2	2.9	4.3	0.0	0.0
800	23.3	32.4	13.5	26.8	33.9	3.4	12.0	9.5	8.9	12.4	3.8	5.7	2.0	9.9
900	22.21	31.0	13.3	26.6	34.3	3.4	12.2	9.8	8.3	11.6	4.2	6.3	5.4	11.2

Table 6. Cumulative Gas Productions and Heating Values

furnace temperature (°C)	cumulative gas production (mol/kg RDF)								heat of combustion (kJ/mol)
	CO	CO_2	H_2	CH_4	C_2H_4, C_2H_2	C_2H_6	C_3H_6	total	
500	6.7	1.2	1.9	0.6	0.2	0.1	0.0	10.6	297
600	6.1	1.6	3.9	1.1	0.2	0.3	0.0	13.2	318
700	5.7	2.1	4.9	1.3	1.3	0.5	0.0	25.7	410
800	4.5	2.6	6.6	2.3	1.7	0.7	0.9	19.4	507
900	5.0	3.0	7.7	2.8	1.9	1.0	1.2	22.5	519

tion and morphology; together with the char yields, these data can also be important to gather some preliminary information on feasibility, operating conditions, and yields of the possible char gasification processes of the RDF.

From Figures 2 and 3 it is clear that the main degradation reactions of the RDF during pyrolysis take place mainly at temperatures lower than 550 °C. This is confirmed by FBR char yields after 60 min, which are almost constant at temperatures higher than 500 °C; less than 2% variation in the solid residue can be observed between 600 and 800 °C. This trend is common to experimental data reported in the literature (Rampling and Hickey, 1988). Furthermore, the constancy of the char yield in conventional pyrolysis processes at temperatures higher than 500 °C is a common feature of many bio-organic materials such as wood and biomass (Koufopanos et al., 1989; Maschio et al., 1994).

Ultimate analyses of chars obtained at various furnace temperatures are reported in Table 4. The almost constant elemental composition of the char between 500 and 800 °C confirms that no significant reaction takes place within the solid in this temperature range, at least for the operating conditions used in present work, which are typical of conventional pyrolysis processes. Between 800 and 900 °C a sudden decrease can be observed in the hydrogen and oxygen content of the solid residue, together with a 5% decrease in the solid residue fraction (see Figure 7), which means a 20% decrease in the char yield. This is reasonably attributable both to high-temperature dehydrogenation of char (as confirmed by the increased hydrogen content of the pyrolysis gases shown in Tables 5 and 6) and to degradation of inorganic fillers (mainly calcium carbonate decarboxylation) present in the RDF (Cozzani et al., 1994).

Figure 8 shows SEM microphotographs of virgin RDF (a) and of the chars obtained at 450 °C (b) and 900 °C (c). It should be recalled that the RDF used in this work has been milled to a fine powder, so that Figure 8a shows the milled RDF. In spite of the fine milling and mixing, the composite and heterogeneous nature of RDF clearly emerges from Figure 8a, where the filamentous structures are probably cellulosic fibers, while the irregular spheroidal particles are mainly attributable to plastic and wood components. Comparison between parts a–c of Figure 8 shows how the macroscopic shape and structure of the RDF is almost unaffected by the pyrolysis process, in spite of the substantial weight loss experienced. While the cellulosic fibers seem to shrink slightly, without the formation of any microporous structure, a moderate increase in the porosity can be inferred from the sponge-like aspect of spheroidal particles that can be noted in Figure 8c. This is confirmed in Figure 9, where the internal surface area of the char is reported as a function of the pyrolysis temperature. The low value of the surface area even at pyrolysis temperatures as high as 900 °C clearly points out that the char obtained from RDF pyrolysis does not have the microporous structure which is typical of coal char obtained under similar operating conditions.

2. Liquid Phases. Two different immiscible condensable fractions were obtained by RDF pyrolysis. One is a high chemical oxygen demand (COD) aqueous phase, which contains mainly low molecular weight organo-oxygen compounds (acids, ketones, and aldehydes). The other is a tar containing a wide variety of high molecular weight organic compounds. This non-aqueous phase tends to solidify as a wax at ambient temperature, and its viscosity increases strongly on exposure to air, due to polymerization processes.

The two condensable fractions were analyzed from a qualitative point of view only. As far as the aqueous phase is concerned, the main organic compounds, determined by gas chromatograph–mass spectrometer analysis after extraction with *n*-pentane and chloroform (Rovatti et al., 1992), were ethanone, 2-propanone, 2-butanone, 1-butanol, acetic acid, cyclopentanone, pentanoic acid, 2-furanone, cyclohexanone, phenol, nonene, and benzoic acid. The tar phase was not analyzed. Literature data are available on the analysis of tars from the conventional pyrolysis of RDFs (Evans and Milne, 1988; Helt and Mallya, 1988), of cellulosic materials (Evans and Milne, 1987; Maschio et al., 1992; Koufopanos, 1986; Fraga et al., 1991), and of polyethylene (Sugimura and Tsuge, 1979; Hodgkin et al., 1982). Tar obtained from the pyrolysis of cellulosic materials is mainly composed of single-ring substituted aromatics, while tar from polyethylene pyrolysis comprises high molecular weight aliphatic hydrocarbons (mainly C_8–C_{23}). A complete screening of the compounds present in the tar obtained from RDF pyrolysis has been obtained by Evans and Milne (1988) by a molecular-beam mass spectrometric technique. The tar obtained from RDF pyrolysis has been found to be composed mainly of oxygenated and single-ring aromatic compounds, formed by the pyrolysis of cellulosic components, and of long-chain aliphatic hydrocarbons, due to degradation of the plastic fraction. Heating values for the tar have been determined by an adiabatic bomb

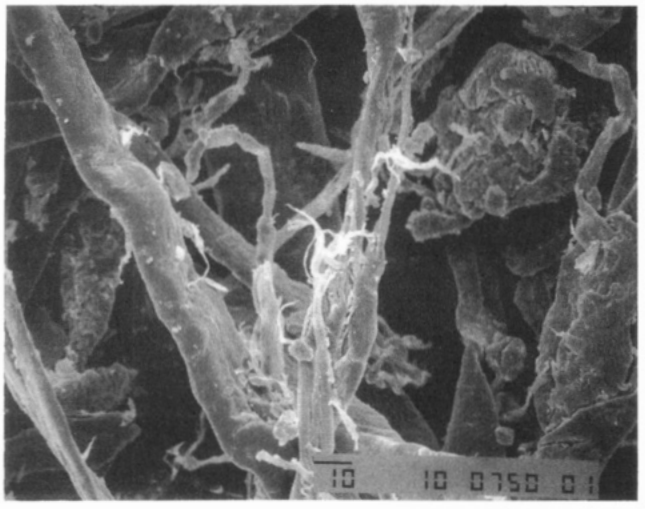

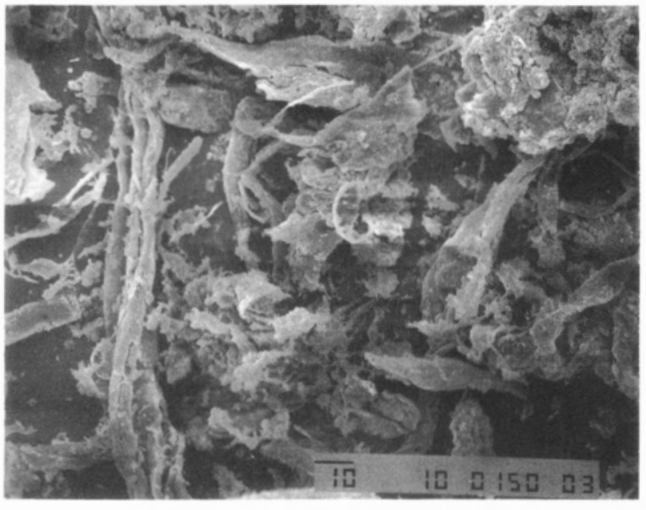

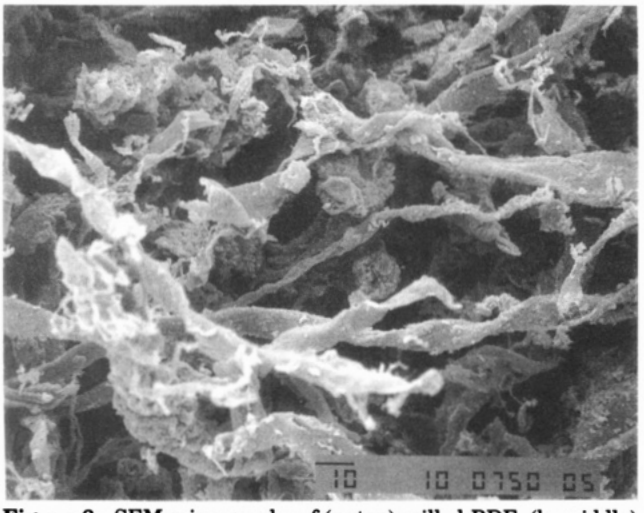

Figure 8. SEM micrographs of (a, top) milled RDF, (b, middle) char after pyrolysis at 450 °C and (c, botttom) char after pyrolysis at 900 °C.

calorimeter, obtained under experimental conditions similar to those of the present work: they ranged between 10 and 20 MJ/kg (Rampling and Hickey, 1988). The density is within the range 900−1100 kg/m^3 (Maschio et al., 1992). The heating value and the rather high density allow the use of the nonaqueous phase obtained by RDF pyrolysis as a quite energetically dense fuel, though some difficulties may arise from its sensitivity to air and temperature, its high viscosity, and its low solubility in apolar organic solvents such as heptane and gasoline. The disposal of the aqueous phase may present environmental problems due to its high COD level.

3. Gases. The gas composition obtained from GC analysis is reported as a function of furnace temperature in Table 5. The calculated cumulative gas production data are reported in Table 6. The table also reports the overall estimated heating value of the pyrolysis gas. All data reported in Table 6 are referred to the product gases considered free of carrier gas.

The gas composition and yields are strongly dependent on the reactor temperature, since the formation of gaseous compounds is the result of a quite complex chemical pathway, where four main phenomena, which can occur simultaneously and independently, are identified. (1) RDF pyrolysis, giving primary incondensable products; (2) heterogeneous interactions between the char and volatiles; (3) vapor-phase tar cracking; and (4) gas-phase reactions between uncondensables and water. In the present work, pyrolysis and secondary interactions between the char and volatiles seem to have a negligible influence on the variations of the gas composition with the reactor temperature. As a matter of fact, comparison of Figures 5 and 6b clearly shows that primary gases are almost fully generated at bed temperatures lower than 550 °C, independent of furnace temperature. Heterogeneous interactions are limited, since during primary volatiles generation the bed temperature is low and the carrier gas sweeps off the volatiles, thus drastically reducing the contact time with the hot char. On the contrary, tar-cracking and other gas-phase reactions seem to have a growing importance on final gas composition as the reactor temperature is increased.

Gaseous products of the overall pyrolysis process consist mainly of carbon dioxide, hydrogen, and carbon monoxide. The content of hydrogen (high-temperature dehydrogenation of char) and carbon dioxide increases at higher reactor temperatures, while that of carbon monoxide decreases. Methane and other light hydrocarbons seem to be present in significant amounts only in the products of the high-temperature runs, thus suggesting that these compounds are mainly arising from secondary homogeneous reactions. The progressive enrichment in hydrogen and hydrocarbons C_{1-4} also causes the overall gas heating value to increase with increasing reactor temperatures.

Overall Kinetics of Gas-Phase Reactions. The wide differences reported in the literature for gases and tar yields obtained from biomass and MSW pyrolysis may be partially attributed to the lack of understanding of the secondary interactions of volatiles, which are strictly dependent on the reactor configuration.

The geometry of the FBR used herein allows for the presence of gas-phase homogeneous reactions of volatiles generated by RDF pyrolysis. As a matter of fact, volatiles are generated by pyrolysis reactions in the wire-mesh sample holder and pass through an extended hot tubular zone before leaving the reactor (see Figure 1). Assuming a plug-flow behavior, the mean residence times in the hot section were evaluated on the basis of the available reactor volume and the measured outlet gas flow rates. The calculated mean residence times are reported as a function of temperature in Figure 10. The temperature of this "homogeneous" section is that of the carrier gas. The time scale which the released pyrolysis primary gases need to reach the furnace wall

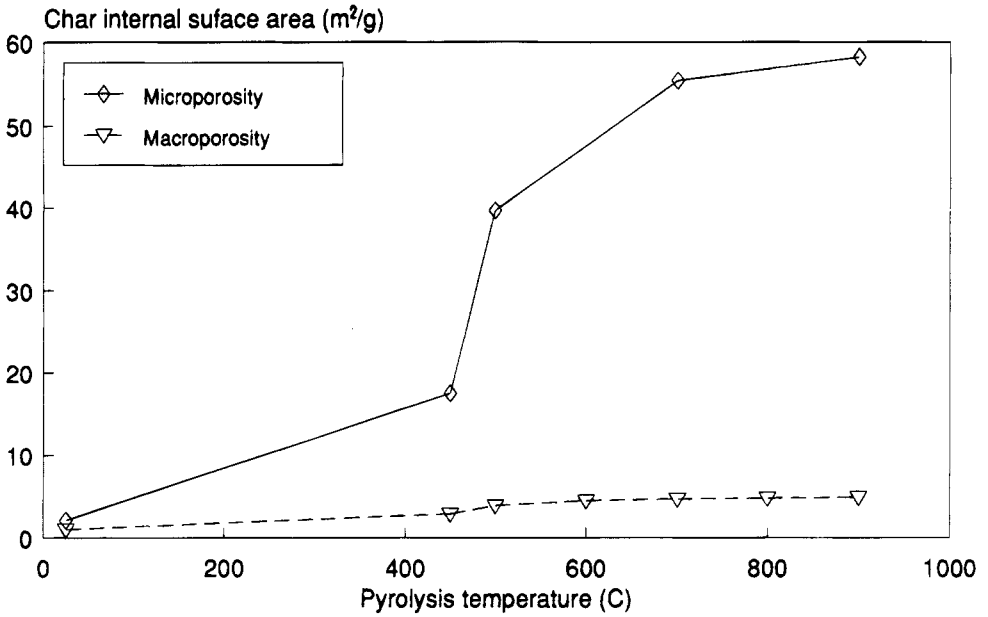

Figure 9. Char surface area after pyrolysis of RDF at different reactor temperatures.

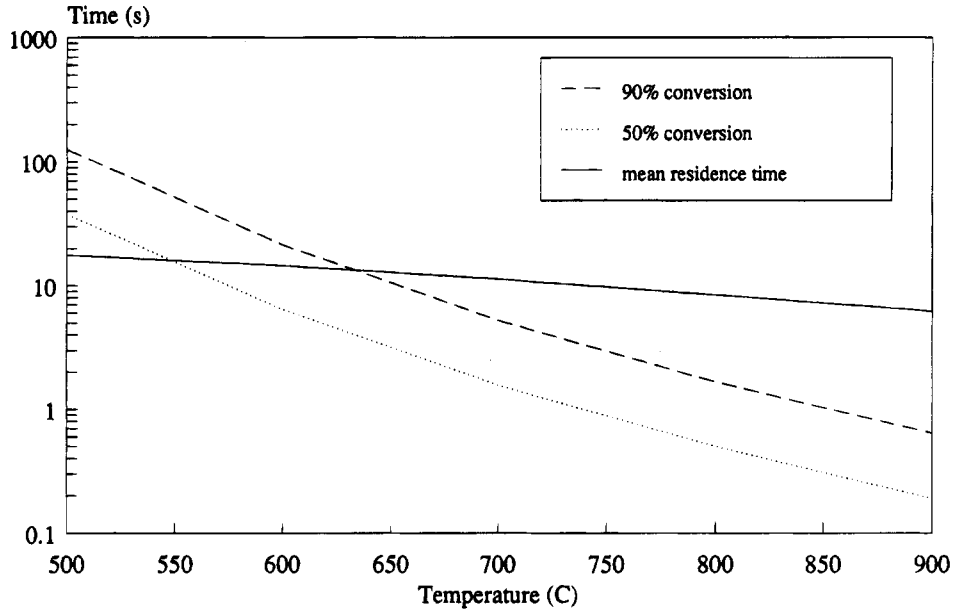

Figure 10. Comparison between volatile residence time in the reactor and characteristic tar-cracking time (time to convert 50%, $\tau_{R,0.5}$, and 90%, $\tau_{R,0.9}$ of tar).

temperature (carrier gas temperature) is, in the laminar flow conditions of present experiments:

$$\tau \simeq (R - r)^2/\alpha \qquad (2)$$

where α is the gas thermal diffusivity (on the order of 20 cm^2/s under the conditions of the experimental runs), R is the reactor inner diameter, and r is the basket outer diameter. Calculated values of τ were less than 5×10^{-2} s under the present conditions, so that gas characteristic heating times are more than 2 orders of magnitude smaller than the residence times in the reactor, thus allowing us to neglect the heating time of the generated volatiles.

In order to verify the possibility of the occurrence of tar-cracking reactions, the single-step model proposed by Boroson et al. (1989) was used herein to evaluate the characteristic tar-cracking times and to compare them with the volatile's residence time in the "homogeneous" reactor section. Even though the kinetic parameters used in the model were obtained for the cracking of tar produced by wood pyrolysis, they seem to be also adequate for this RDF, as will be discussed in the following. Figure 10 reports a semiquantitative comparison between the estimated mean residence times and the calculated residence times required to convert 50% and 90% of crackable tar as a function of temperature. The temperatures for which a substantial change in the tar yield is found (furnace temperature of 600 °C, which means a gas mean temperature of about 580 °C) are those at which tar cracking starts to be effective, due to the volatile's residence times greater than the characteristic reaction times (Figure 10).

The main problem in determining the influence of gas-phase tar-cracking reactions on final product yields in the FBR used in the present work is that it is not possible to directly measure the primary yields of gases and tar generated by the pyrolysis process in the absence of gas-phase reactions. Nevertheless, primary yields can be estimated by a working hypothesis. From

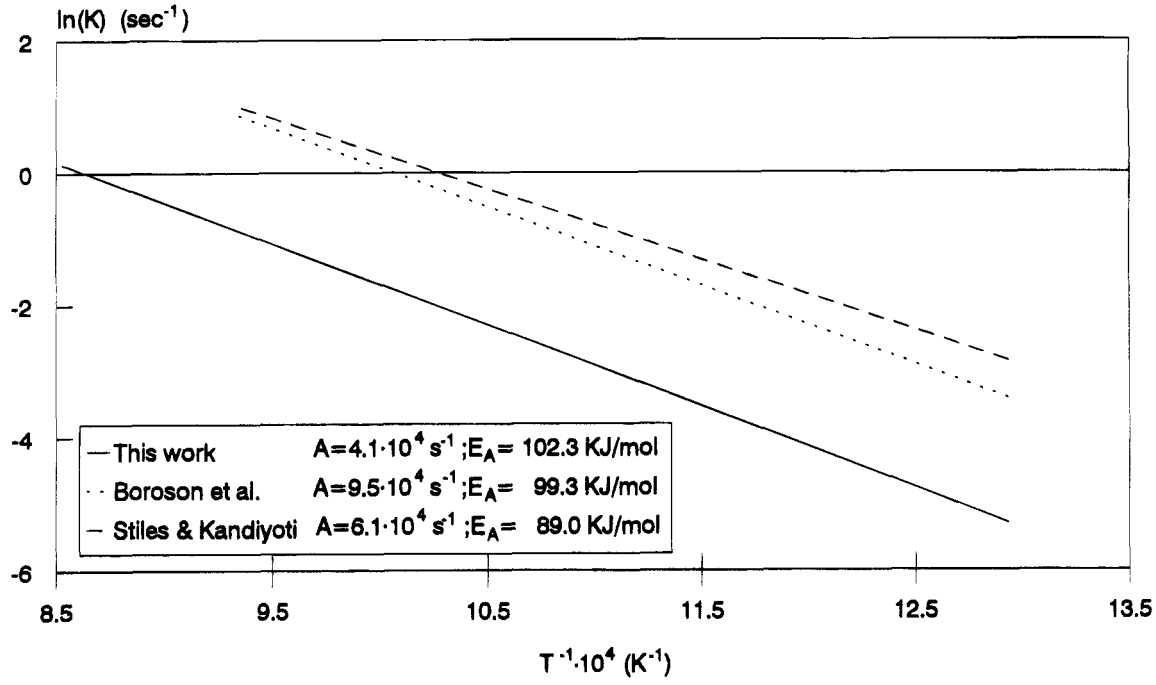

Figure 11. Comparison of kinetic data for the homogeneous tar-cracking process.

the comparison of fixed bed temperature–time curves and of gas evolution rates (see Figures 5 and 6b) it clearly emerges that volatiles are almost fully generated at bed temperatures lower than 600 °C even at the maximum furnace temperature (900 °C). This suggests that in the experimental system used herein, the effect of the furnace temperature on the primary pyrolysis products is negligible. Since tar-cracking reactions are almost absent at 500 °C (Evans and Milne, 1987; Stiles and Kandiyoti, 1989; Bingyan et al., 1992), as also shown in Figure 10, the volatiles obtained in the FBR from the 500 °C run may be regarded as primary pyrolysis products.

It was then possible to estimate indicative values for the kinetic parameters of the tar-cracking reactions. A single-step first-order Arrhenius kinetic rate equation was used to correlate the experimental data. This choice seems the most adequate, since this kinetic model has been extensively and successfully used for the correlation of overall gas-phase conversion kinetics of volatiles generated by other complex starting materials such as wood (Boroson et al., 1989) and coal (Howard, 1981). Furthermore, first-order reactions are important pathways in the gas-phase cracking of high-molecular weight species, such as cracking of tars to lower molecular weight species. The kinetic equation used for data fitting was

$$dC_i/dt = A_i e^{E_{a,i}/RT}(C_i^* - C_i) \qquad (3)$$

where A_i is the frequency factor for material i, $E_{a,i}$ is the apparent activation energy, R is the universal gas constant, T is the reactor temperature, C_i is the yield of material i at time t (final yields at the estimated mean residence times were used), C_i^* is the ultimate value of C_i at high temperature, determined experimentally.

Thus a first-order dependency of the difference between the ultimate (minimum) tar yield and the total unconverted tar is inferred for tar-cracking reactions, while gas formation reactions had a first-order dependence on the difference between the ultimate (generally maximum) gas yield and the gas yield at time t. The definition of the ultimate tar and gas yields is clearly only a working definition, resulting from the range of reactor temperatures and residence times used herein, since at higher reactor severities relevant changes may be expected in the values of ultimate yields.

The initial condition used to integrate eq 3 was, independently of the furnace temperature used in experimental run:

$$C_i(t=0) = C_{i,500} \qquad (4)$$

where $C_{i,500}$ is the final yield of material i obtained from the 500 °C run.

Approximately five runs for each reactor temperature were performed to obtain reliable values of the product yields. The frequency factor and the apparent activation energy were obtained by a least-squares minimization technique.

The kinetic parameters obtained should be considered only as indicative estimates, since the assumptions made lead to an oversimplified kinetic model. However, this kind of approach, based on a drastic lumping of both chemical reactions and reacting species involved in the process, has been widely used in the literature and has given fruitful results. The logarithm of the kinetic constant K obtained for the overall gas-phase tar-cracking reaction is plotted versus the reciprocal of the temperature (Arrhenius plot) in Figure 11, and a comparison is made with the literature data obtained for wood (Boroson et al., 1989) and MSW (Stiles and Kandiyoti, 1989) pyrolysis. Since a different kinetic model was used by Stiles and Kandiyoti, the Arrhenius plot and kinetic parameters in Figure 11 were evaluated by fitting their experimental data to the model used herein. Table 7 reports the values of the kinetic parameters obtained for the secondary homogeneous gas generation reactions.

A quite good agreement is shown between the values of the activation energies and frequency factors reported in Figure 11, in spite of the quite different starting materials used (RDF, wood, and MSW) and of the differences in reactor systems. This is possibly due to

Table 7. Kinetic Data for Homogeneous Single Gas Production

	A (s^{-1})	E_a kJ/mol	σ^a
CO	1.6×10^3	76.5	0.21
CO_2	1.3×10^3	73.5	0.09
H_2	2.0×10^2	57.6	0.10
CH_4	7.9×10^2	70.5	0.27
C_2H_4	3.2×10^4	96.7	0.16
C_2H_6	2.5×10^2	62.1	0.01

[a] Standard deviation.

the presence of common "primary reacting species", such as cellulose and lignin, which may result in a similar composition of the reactive fraction of primary volatiles generated by the pyrolysis process.

Conclusions

The pyrolysis behavior of a refuse-derived fuel (RDF) under heating conditions typical of conventional pyrolysis processes was investigated. Comparison of TGA and DSC data for the RDF and its components demonstrates quite well that the behavior of the RDF during pyrolysis may be considered as the sum of the separate behaviors of each key component. This conclusion is likely to hold at least for the conditions of present experiments, i.e., relatively small particles and low heating rates.

The pyrolysis products obtained in a laboratory-scale fixed bed reactor at temperatures between 500 and 900 °C were identified and characterized by different experimental techniques. Char, tar, water, and gas yields were independently determined, with a mass balance better than 95%. The char yield was quite low and almost independent of temperature. The yields of both aqueous and nonaqueous liquid phases were found to decrease with the operating temperature in the range 600–900 °C. This depletion was associated with the evident increase of the gas fraction at furnace temperatures higher than 600 °C, and it has been related to the occurrence of tar-cracking reactions in the homogeneous phase.

Gas composition and yields were strongly dependent on the reactor temperature. The content of hydrogen and carbon dioxide increased at higher reactor temperatures, as that of carbon monoxide decreased. Methane and other light hydrocarbons were found to be present in significant amounts only at high temperatures, thus suggesting that these compounds are mainly arising from secondary homogeneous reactions. The progressive enrichment in hydrogen and hydrocarbons C_{1-4} also causes the overall gas heating value to increase with increasing reactor temperatures.

Since the formation of gaseous compounds is the result of a quite complex chemical pathway, where different phenomena are involved, it seems difficult to draw general conclusions on the dependence of the product yields of volatiles (gases, tar, and water) on the temperature for each primary reacting species, as yields critically depend on reactor operating conditions (heating rates and residence times). As a matter of fact, wide differences are reported in the literature for yields of gases and tar obtained from biomass and MSW pyrolysis, which may be partially attributed to the lack of understanding of the secondary interactions of volatiles,which are strictly dependent on the reactor configuration.

The kinetic parameters obtained in this study should be considered only indicative estimates, since the assumptions made lead to an oversimplified kinetic model. However, a quite good accordance was found between the values of the activation energies and the frequency factors evaluated in the present study and those from literature data, in spite of the quite different starting materials used (RDF, wood, and MSW) and of the differences in reactor systems. This is possibly due to the presence of common "primary reacting species", such as cellulose and lignin, which may result in a similar composition of the reactive fraction of primary volatiles generated by the pyrolysis process.

Finally, it is worthwhile to note that the low char yield and the high volatile content of the RDF also point out the crucial role of the pyrolysis stage in gasification processes.

Literature Cited

Agrawal, R. K.; Gandhi, F.; McCluskey, R. J. Low pressure pyrolysis of newsprint. Product formation. *J. Anal. Appl. Pyrolysis* **1984**, *6*, 325.

Antal, J. M., Jr. Effect of reactor severity on the gas phase pyrolysis of cellulose- and Kraft lignin-derived volatile matter. *Ind. Eng. Chem., Prod. Res. Dev.* **1983**, *22*, 166.

Antal, J. M., Jr. Biomass pyrolysis, a review of the literature; part II: lignocellulosic pyrolysis. *Adv. Solar Energy* **1985**, *2*, 175.

Bergui, G. Cinetica del tar-cracking nella pirolisi di materie plastiche. *Chem. Eng. Thesis*, Universita' degli Studi di Genova, Genova, 1994.

Bilbao, R.; Arauzo, J.; Millera, A. Kinetics of thermal decomposition of cellulose. Part I. Influence of experimental conditions. *Thermochim. Acta* **1987**, *120*, 121.

Bilbao, R.; Millera, A.; Arauzo, J. Kinetics of weight loss by thermal decomposition of xylan and lignin. Influence of experimental conditions. *Thermochim. Acta* **1989**, *143*, 137.

Bingyan, X.; Chuangzhi, W.; Zhengfen, L.; Xiguang, Z. Kinetic study on biomass gasification. *Solar Energy* **1992**, *49* (3), 199.

Boroson, M. L.; Howard, J. B.; Longwell, J. P.; Peters, W. A. Products yields and kinetics from the vapor phase cracking of wood pyrolysis tars. *AIChE J.* **1989**, *35*, 120.

Buekens, A. G.; Schoeters, J. G. European experience in the pyrolysis and gasification of solid wastes. *Conserv. Recycl.* **1986**, *9*, 253.

Capart, R.; Fagbemi, L.; Gelus, M. Wood pyrolysis: a model including thermal effect of the reaction. *Energy from Biomass*; Palz, W., Coombs, J., Hall, D. O., Eds.; Elsevier: London, 1986; p 842.

Chan, W. R.; Kelbon, M.; Krieger-Brockett, B. Single particle biomass pyrolysis; correlations of reaction products with process conditions. *Ind. Eng. Chem. Res.* **1988**, *27*, 2261.

Cozzani, V.; Petarca, L.; Tognotti, L. Devolatilization and Pyrolysis of Refuse Derived Fuels: Characterization and Kinetic Modeling by a Thermogravimetric and Calorimetric Approach. *Fuel* 1994, in press.

Di Blasi, C. Modeling and simulation of combustion processes of charring and non-charring solid fuels. *Prog. Energy Combust. Sci.* **1993**, *19*, 71.

Eggen, A. C. W.; Kraatz, R. Gasification of solid waste in fixed beds. ASME Winter Annual Meeting, New York, 1974.

Ekstrom, C.; Rensfelt, E. Studsvik CFBG gasification and gas cleaning technology. *Energy Biomass Wastes* **1989**, *12*, 891.

Evans, R. J.; Milne, T. A. Molecular characterization of the pyrolysis of biomass. 1. Fundamentals. *Energy Fuels* **1987**, *1*, 123.

Evans, R. J.; Milne, T. A. Mass spectrometric studies of the relationship of pyrolysis oil composition to formation mechanisms and feedstock composition. *Research in Thermochemical Biomass Conversion*; Bridgwater, A. V., Kuester, J. L., Eds.; Elsevier: London, 1988; p 265.

Fraga, A. R.; Gaines, A. F.; Kandiyoti, R. Characterization of biomass pyrolysis tars produced in the relative absence of extraparticle secondary reactions. *Fuel* **1991**, *70*, 803.

Grassie, N.; Scott, G. *Polymer degradation and stabilization*; Cambridge University Press: Cambridge, 1985.

Hajaligol, M. R.; Howard, J. B.; Longwell, J. P.; Peters, W. A. Product composition and kinetics for rapid pyrolysis of cellulose. *Ind. Eng. Chem., Process Des. Dev.* **1982**, *21*, 457.

Hodgkin, J. H.; Galbraith, M. N.; Chong, Y. K. Combustion products from burning polyethylene. *J. Macromol. Sci., Chem.* **1982**, *A17* (1), 35.

Howard, J. B. Fundamentals of coal pyrolysis and hydropyrolysis. *Chemistry of coal utilization, 2nd suppl. vol.*; Elliot, M. A., Ed.; Wiley: New York, 1981; chapter 12.

Iida, T.; Nakanishi, M.; Goto, K. Investigation on poly(vinylchloride). II pyrolysis of chlorinated polybutadienes as model compounds for poly(vinylchloride). *J. Polym. Sci., Polym. Chem. Ed.* **1975**, *73*, 1381.

Khalturinskii, N. A. High temperature pyrolysis of polymers. *J. Therm. Anal.* **1987**, *32*, 1675.

Kojima, E.; Miao, Y.; Yoshizaki, S. Pyrolysis of cellulose particles in a fluidized bed. *J. Chem. Eng. Jpn.* **1991**, *24*, 8.

Koufopanos, C. A. Studies on the pyrolysis and gasification of biomass. Final report of grant period 1983–1986, Commission European Communities, 1986.

Koufopanos, C. A.; Maschio, G.; Lucchesi, A. Kinetic modelling of the pyrolysis of biomass and biomass components. *Can. J. Chem.Eng.* **1989**, *67*, 75.

Koufopanos, C. A.; Papayannakos, N.; Maschio, G.; Lucchesi, A. Modelling of the pyrolysis of biomass particles. Studies on kinetics, thermal and heat transfer effects. *Can. J. Chem. Eng.* **1991**, *69*, 907.

Jellinek, H. H. G. Thermal degradation of polystyrene and polyethylene. Part III. *J. Polym. Sci.* **1949**, *4*, 13.

Lai, W. C.; Krieger-Brockett, B. Volatiles release rates and temperatures during large particle Refuse Derived Fuel - Municipal Solid Waste devolatilization. *Combust. Sci. Technol.* **1992**, *85*, 133.

Madorski, S. L. Rates of thermal degradation of polystyrene and polyethylene in a vacuum. *J. Polym. Sci.* **1952**, *9*, 133.

Mallya, N.; Helt, J. E. Effects of feedstock components on municipal solid waste pyrolysis. *Research in Thermochemical Biomass Conversion*; Bridgwater, A. V., Kuester, J. L., Eds.; Elsevier: London, 1988; p 111.

Maschio, G.; Koufopanos, C.; Lucchesi, A. Pyrolysis, a promising route for biomass utilization. *Bioresource Technol.* **1992**, *42*, 219.

Maschio, G.; Lucchesi, A.; Stoppato, G. Production of syngas from biomass. *Bioresource Technol.* **1994**, *48*, 119.

Muhlen, H. J.; Wanzl, W.; Van Heek, K. H. Characterization of carbon containing materials with respect to pyrolysis and gasification. *EEC Conference on Pyrolysis and Gasification*; Ferrero et al., Eds; Elsevier: London, 1989; p 72.

Murphy, M. L. Gasification of RDF: a practical look at the technology. Proceedings of Waste to energy, New Orleans, 1989.

Oakes, W. G.; Richards, R. B. The thermal degradation of ethylene polymers. *J. Chem. Soc., London* **1949**, *619*, 2929.

Rampling, T. W.; Hickey, T. J. The laboratory characterization of Refuse Derived Fuel. Warren Spring Lab. Rep. No.ETSU-B-1161; Crown Copyright, 1988.

Rensfelt, E.; Ekstrom, C. Fuel gas from municipal waste in an integrated circulating fluid bed gasification/gas cleaning process. Energy from biomass and wastes, New Orleans, 1988.

Rinker, F. G. Solid waste gasification and energy utilization. *Thermal conversion of solid wastes and biomass*; ACS Symposium Series 130; American Chemical Society: Washington, DC, 1980; p 291.

Roberts, A. F. Review of kinetics data for the pyrolysis of wood and related substances. *Combust. Flame* **1970**, *14*, 261.

Rovatti, M.; Bisi, M.; Palazzi, E.; Ferraiolo, G. Pirolisi di combustibile derivato dai rifiuti solidi urbani (MRDF). (Pyrolysis of Fuel Derived from Municipal Solid Wastes.) *Acqua aria* **1992**, *2*, 127.

Scott, D. S.; Piskorz, J.; Bergougnou, M. A.; Graham, R.; Overend, R. P. The role of temperature in the fast pyrolysis of cellulose and wood. *Ind. Eng. Chem. Res.* **1988**, *27*, 8.

Stahlberg, P.; Kurkela, E.; Filen, H.; Salo, K. Updraft gasification of waste fuels. *EEC Conference on Pyrolysis and Gasification*; Ferrero et al., Eds; Elsevier: London, 1989.

Stiles, H. N.; Kandiyoti, R. Secondary reactions of flash pyrolysis tars measured in a fluidized bed pyrolysis reactor with some novel design features. *Fuel* **1989**, *68*, 275.

Sugimura, Y.; Tsuge, S. Pyrolysis-hydrogenation glass capillary gas chromatographic characterization of polyethylenes and ethylene-α-olefin copolymers. *Macromololecules* **1979**, *12*, 512.

Vigil, S. A.; Bartley, D. A.; Healy, R.; Tchobanoglous, G. Operation of a downdraft gasifier fueled with source-separated solid waste. *Thermal conversion of solid wastes and biomass*; ACS Symposium Series 130; American Chemical Society: Washington, DC, 1980; p 257.

Ward, S. M.; Braslaw, J. Experimental weight loss kinetics of wood pyrolysis under vacuum. *Combust. Flame* **1985**, *61*, 261.

Received for review April 19, 1994
Revised manuscript received October 5, 1994
Accepted February 23, 1995[⊗]

IE940256B

[⊗] Abstract published in *Advance ACS Abstracts,* April 15, 1995.